Subcellular clustering of a putative c-di-GMP-dependent exopolysaccharide machinery affecting macro colony architecture in *Bacillus subtilis*

Patricia Bedrunka and Peter L. Graumann*

LOEWE SYNMIKRO, LOEWE Center for Synthetic Microbiology and Department of Chemistry, Philipps University Marburg, Hans-Meerwein Strasse, 35043 Marburg, Germany

*Corresponding author
Phone + 49 (0)6421 2822210
Fax + 49 (0)6421 2822262
graumanp@uni-marburg.de

Originality-Significance Statement

A) Identification of a novel putative exopolysaccharide machinery in *Bacillus subtilis*

B) New function of YdaJ and YdaK in *B. subtilis*

C) Potential new tool to study c-di-GMP signaling in *Bacillus subtilis*

This article has been accepted for publication and undergone full peer review but has not been through the copyediting, typesetting, pagination and proofreading process which may lead to differences between this version and the Version of Record. Please cite this article as an 'Accepted Article', doi: 10.1111/1758-2229.12496

Abstract

The structure of bacterial biofilms is predominantly established through the secretion of extracellular polymeric substances (EPS). We show that *Bacillus subtilis* contains an operon (*ydaJ-N*) whose induction leads to increased Congo Red staining of biofilms and strongly altered biofilm architecture, suggesting that it mediates the production of an unknown exopolysaccharide. Supporting this idea, overproduction of YdaJKLMN leads to cell clumping during exponential growth in liquid culture, and also causes colony morphology alterations in wild type cells, as well as in a mutant background lacking the major exopolysaccharide of *B. subtilis*. The first gene product of the operon, YdaJ, appears to modify the overproduction effects, but is not essential for cell clumping or altered colony morphology, while the presence of the c-di-GMP receptor YdaK is required, suggesting an involvement of second messenger c-di-GMP. YdaM, YdaN and YdaK colocalize to clusters predominantly at the cell poles and are statically positioned at this subcellular site, similar to other exopolysaccharide machinery components in other bacteria. Our analysis reveals that *B. subtilis* contains a static subcellular assembly of an EPS machinery that affects cell aggregation and biofilm formation.

Introduction

In natural environments, microbes are predominantly organized in sessile multicellular communities called biofilms (Costerton et al., 1995; Shapiro, 1998). These assemblages consist of distinct subpopulations of specialized cells which exhibit spatial and temporal organization during their coexistence within the community that is encapsulated by a protective extracellular matrix (ECM). In the process of biofilm development for instance, a fraction of the population differentiates into matrix-producing cells in response to external and internal signals (Stewart and Franklin, 2008; Vlamakis et al., 2013). The extracellular matrix synthesized by those specialized cells, consists of extracellular polymeric substances (EPS), encompassing mainly polysaccharide, proteins and nucleic acids and can account for 90 % of the biomass (Flemming and Wingender, 2010). Extracellular matrix components are indispensable for biofilm formation and conservation as their nature determines the physicochemical and biological qualities of a biofilm and ensures the structural and functional integrity of the community.

Undomesticated strains of the Gram-positive soil-dwelling bacterium *Bacillus subtilis* such as NCIB3610, are able to form floating biofilms at air-liqiud interfaces (pellicles), structured colony biofilms on semi-solid agar surfaces and are furthermore capable of colonizing plant roots (Branda et al., 2001; Cairns et al., 2014). Laboratory strains such as 168 and PY79 have largely lost the ability to spread on semi solid agar and to form biofilms as a consequence of domestication (Zeigler et al., 2008; McLoon et al., 2011).

The formation of those complex surface-associated communities depends substantially on the synthesis and secretion of EPS including predominantly the major protein components TasA/TapA which is proposed to constitute an amyloid fibre network (Branda et al., 2006; Romero et al., 2010), the surface-active protein BslA, considered as a bacterial hydrophobin (Kobayashi and Iwano, 2012; Hobley et al., 2013) and particularly exopolysaccharides.

Several studies have demonstrated the importance of the 15 gene-long *epsA-O* cluster concerning biofilm formation in *B. subtilis in vitro* and *in planta* (Marvasi et al., 2010). The chemical composition of the polysaccharide produced by the products of this operon apparently depends on growth conditions/substrate availability and needs to be further clarified (Cairns et al., 2014; Roux et al., 2015).

Furthermore, *B. subtilis* is able to synthesize the exopolysacharide levan, a homopolymer of fructose, via the *epsA-O* adjacent *sacB-yveB-yveA* operon (Dogsa et al., 2013) and the extracellular amino acid polymer γ-polyglutamate (Morikawa et al., 2006; Scoffone et al., 2013).

In this study, we address the question whether an additional putative exopolysaccharide synthesis operon (*ydaJKLMN*) contributes to ECM- and thus biofilm formation in *B. subtilis* under laboratory conditions. Most interestingly, the second gene product YdaK encodes for a putative c-di-GMP receptor (Chen et al., 2012; Gao et al., 2013) indicating a new function of this second messenger in *B. subtilis*.

The second messenger bis-(3′–5′)-cyclic dimeric guanosine monophosphate (c-di-GMP) is a key regulator in the transition between motile and non-motile lifestyles of bacteria (Hengge, 2009). Generally, increased levels of c-di-GMP promote sessile lifestyle and biofilm formation, whereas motility and single cell behavior is inhibited under these circumstances (Simm et al., 2004; Jenal and Malone, 2006). The synthesis and hydrolysis of c-di-GMP is mediated by two sets of enzymes. It is synthesized by diguanylate cyclases (DGCs), which harbor a conserved GGDEF domain, from two molecules GTP and is degraded by specific phosphodiesterases (PDEs) containing either a conserved EAL or HD-GYP domain, giving rise to the linear dinucleotide 5′-phosphoguanylyl-(3′,5′)-guanosine (pGpG).

The GGDEF domain of the transmembrane protein YdaK carries a degenerated GG(D/E)EF signature motif (SDERI) and was shown to be deficient in c-di-GMP synthesis in. However, the 4 TM protein is able to bind c-di-GMP with moderate affinity via its soluble C-terminal GGDEF domain, likely at the so called I-site (signature motif RxxD, allosteric product inhibition site in active DGCs) but it is incapable of modulating swarming motility as demonstrated for DgrA, a conserved PilZ-domain c-di-GMP receptor (Chen et al., 2012; Gao et al., 2013).

Because c-di-GMP is known as a transcriptional and posttranslational regulator of different bacterial exopolysaccharide machineries (Liang, 2015), we were interested whether YdaK as a degenerated GGDEF-TM protein would be able to exert control over genes encoded within the same operon, as PelD from *P. aeuruginosa* (Lee et al., 2007; Liang, 2015) and PssE from *L. monocytogenes* (Chen et al., 2014; Koseoglu et al., 2015). We were also interested in testing the subcellular localization of the products of the *yda* operon. Bacterial exopolysaccharide machineries or components of these have been reported to localize to the cell poles for several species including *A. tumefaciens* (Xu et al., 2013), *E. coli* (Le Quere and Ghigo, 2009) and *S. coelicolor* (Xu et al., 2008). Additionally, the components of the polyketide bacillaene synthase cluster at a single site within *B. subtilis* cells (Straight et al., 2007) showing that multicomponent enzyme complexes can cluster and form an enzymatic megacomplex.

Results

The *ydaJKLMN* operon in *B. subtilis* encodes for a putative exopolysaccharide synthesis operon and contains a gene, *ydaK*, encoding a potential c-di-GMP binding protein

The potential c-di-GMP receptor YdaK is encoded within a transcriptional unit, harboring four additional genes called *ydaJ*, *ydaL*, *ydaM* and *ydaN*. Condition-dependent transcription profiles (tiling microarray data obtained by (Nicolas et al., 2012)) of single genes of the cluster and of its 5´ upstream region (Fig. S1) revealed co-transcription of these genes under various different laboratory conditions, implying that these genes are under the control of the same promotor. The corresponding genes were assigned to the SigB regulon (alternative stress sigma factor in *B. subtilis*), which is reflected in the upregulated transcription of *ydaJKLMN* elements upon stress treatment such as heat, ethanol and high salt, and in the upregulation during germination and notably also during exponentially growth in rich medium supplemented with glucose (Nicolas et al., 2012).

It is interesting to note that the *yda* operon is absent from the genome of laboratory *B. subtilis* strain PY79, because it is part of an approximately 17 kb-long deletion occurring in this domesticated strain (Zeigler et al., 2008). The reason for this deletion, encompassing the *yda* operon and 8 further open reading frames, is unknown. However, the genomes of the strains *B. subtilis* 168 and NCIB 3610 do encode this operon.

Based on bioinformatic analysis of the corresponding elements (for a detailed description see supplementary material Text S1 and Fig. S2A), we hypothesize that the *ydaJKLMN* operon codes for an exopolysaccharide machinery, which is upregulated during exponential growth and various stress conditions and may be regulated by the second messenger c-di-GMP.

Overexpression of *ydaJKLMN* or of *ydaKLMN* leads to increased staining of Congo Red

Deletion or overproduction of YdaK alone had no observable effects under laboratory conditions concerning biofilm formation and motility in *B. subtilis* (Gao et al., 2013). In order to provoke a detectable cellular output by means of extracellular matrix production, we opted to overexpress the entire *ydaJKLMN* unit in three *B. subtilis* strains individually: in the laboratory strain *B. subtilis* 168, in its biofilm-proficient ancestor NCIB3610 and in a biofilm-deficient (*epsH*-) mutant derived from strain NCIB 3610 (*epsH*::*tet*, strain DS9259). Extracellular matrix production was examined by Congo Red (CR) staining and by visual inspection of biofilm formation of *B. subtilis* macro colonies, as reported previously for different bacterial species (Robledo et al., 2008; Romero et al., 2010). Additionally, we

wondered whether YdaJ, product of the first gene within the operon and putative extracellularly-acting endoglucanase, is required for the predicted function (ECM production). Its homolog PssZ (28 % identity, BlastP) is dispensable for extracellular polysaccharide synthesis, mediated by the PssABCDE machinery in *L. monocytogenes* (Koseoglu et al., 2015). Considering this, we decided to generate two constructs mediating the overexpression of the entire transcriptional unit and of a *ydaJ*-lacking variant at the native locus respectively. We used the integrative vector pSG1164 (Lewis and Marston, 1999) and cloned the 5´ end of *ydaJ* or of *ydaK,* respectively, under the control of the plasmid-encoded xylose promotor, resulting in recombinant plasmids pSG1164-PB53 (P_{xyl}-*ydaJKLMN*) and pSG1164-PB55 (P_{xyl}-*ydaJKLMN*). These constructs were inserted into the respective *B. subtilis* genomes by Campbell-like recombination (Campbell et al., 1977). The resulting strains carry a partial gene of *ydaJ* or of *ydaK,* respectively, and the whole *ydaJKLMN* operon or the operon lacking full-length *ydaJ* under the control of the xylose-dependent promoter (see experimental procedure Text S2 and Fig. S2C).

The property of Congo Red accumulation on solid medium has been frequently associated with the production of extracellular matrix components, such as amyloid fibers or cellulose, in various Gram negative and positive bacteria (Friedman and Kolter, 2004; Solano et al., 2009; Chen et al., 2014). Interestingly, we found that both overexpression mutants are able to accumulate CR to a visually greater extent than wild type cells (Fig. 1A). The laboratory strain 168 exhibits no CR-binding and reveals flat and less structured colony morphology in comparison to both overproduction strains. Colonies carrying the plasmid pSG1164-PB53 (strain 168-PB53, P_{xyl}-*ydaJKLMN*) and pSG1164-PB55 (strain 168-PB55, P_{xyl}-*ydaKLMN*) respectively, display a strikingly distinct morphology on CR agar plates containing the inducer xylose compared to the non-induced colonies.

Overexpression of *ydaJKLMN* (168-PB53) as well as of *ydaKLMN* (168-PB55) results in the formation of red irregularly branched wrinkles in the center of the colony, and overall enhanced CR-binding, especially at the outlines of the inoculation area, which indicates a significant difference in extracellular matrix composition between the parental wild type and both overproduction strains. Those wrinkled phenotypes do not occur on indicator plates without xylose (Fig. 1A).

Wrinkled colony morphology and CR-binding has been linked to cell aggregation phenotypes in Gram-negative and positive bacteria (Solano et al., 2009; Koseoglu et al., 2015). We could also observe such aggregation effects (Fig. 1A, Fig. S3), which we quantified by spectrophotometry determining the OD_{600} of induced cultures after 90 min of

settling (Fig. S3). Both overproduction strains, 168- PB53 (P_{xyl}-*ydaJKLMN*) and 168- PB55 (P_{xyl}-*ydaJKLMN*), showed a significant decrease in optical density compared to wild type *B. subtilis* 168 cells, reflecting increased levels of aggregation, although the level of aggregation was visibly enhanced when only *ydaKLMN* (168-PB55) was overexpressed, in comparison to *ydaJKLMN* (168-PB53) overexpression (Fig. 1A, Fig. S3).

Because an overexpression of *ydaKLMN* missing *ydaJ* coding for a putative glycosyl hydrolase (GH8), resulted in a similar CR binding phenotype as the overexpression of the complete operon, we conclude that the gene product of *ydaJ* is not involved in the synthesis of the unknown polysaccharide but possibly in a post-polymerization modification reaction similar to that of PssZ in *L. monocyotogenes*, which acts outside of the bacterial cell membrane and is not essential for EPS production (Koseoglu et al., 2015). This is further supported by the observation that an overexpression of *ydaJ* from the ectopic *amyE* locus along with an overexpression of *ydaKLMN* (original locus) results in enhanced CR binding, but wrinkle formation and aggregation was completely abolished (strain 168-PB55+15, Fig 1A). We speculate that YdaJ partially degrades or modifies the putative exopolysaccharide produced by YdaKLMN.

Overexpression of *ydaJKLMN* or of *ydaKLMN* alteres morphology of *B. subtilis* macro colonies on biofilm-promoting medium

Next, we wondered whether an overexpression of *ydaJKLMN* or of *ydaKLMN* alters the morphology of biofilm colonies of the undomesticated wild type strain NCIB3610 known to exhibit "multicellular" behavior by forming robust and complex macro colonies on a biofilm-inducing solid medium {MSgg, minimal salts with glycerol and glutamate, (Branda et al., 2001)}. In order to investigate the role of *ydaJKLMN* in terms of biofilm formation, the two above-described recombinant plasmids pSG1164-PB53 and pSG1164-PB55 were introduced into the *B. subtilis* NCIB3610 genome individually (strains NCIB3610-PB53, -PB55) and biofilm formation was assessed using solid MSgg medium supplemented with CR/CB in the presence or absence of xylose. Additionally, we included a NCIB3610-derived *ydaK* deletion mutant DS9289 (Gao et al., 2013) in our study. Representative images of the corresponding strains are depicted in Fig. 1B.

In good agreement with previous observations, the wild type strain displayed complex macro colony architecture (Asally et al., 2012), which was not altered by the addition of xylose under these conditions. The overexpression of *ydaJKLMN* (NCIB3610-PB53, P_{xyl}-*ydaJKLMN*) resulted in an inhibited surface spreading behavior and additionally in the

formation of an elevated and extended central ring structure stained with CR/CB, similar to that seen in the 168 background (Fig. 1A). This reduced colony expansion phenotype was even more pronounced in macro colonies that overproduced the machinery lacking the putative glycosyl hydrolase YdaJ (strain NCIB3610-PB55; P_{xyl}-*ydaKLMN*; Fig. 1B). Furthermore, a different wrinkle pattern in the initial central inoculum area can be observed displaying more crowded, irregular and thick ridges, compared to the wild type strain and the overproduction strain NCIB3610-PB53 (P_{xyl}-*ydaJKLMN*). While an overproduction causes strong phenotypes on biofilm-promoting medium, the deletion of one component, such as *ydaK,* has only very mild effects (Fig. 2B, strain DS9289, Δ*ydaK*), as already previously reported by Gao *et al*., 2013, suggesting a minor role of the *ydaJKLMN* operon with respect to biofilm formation under standard laboratory conditions.

Overexpression of *ydaKLMN* results in wrinkle formation and CR-staining in an *epsH* deficient biofilm mutant

The production of exopolysaccharides and other extracellular matrix components is crucial for the development of biofilms in many bacterial species. This is also true for the undomesticated *B. subtilis* strain NCIB3610, which harbors besides the *ydaJKLMN* cluster a 15-gene polysaccharide operon (*epsA-O*), encoding (at least partially) an EPS biosynthetic machinery that is thought to synthesize the extracellular compound poly-N-acetylglucosamine. This machinery is responsible for complex colony architecture (Branda et al., 2001; Branda et al., 2006; Nagorska et al., 2010; Roux et al., 2015). A deletion of *epsH* (strain DS9259, *epsH*::*tet*) results in flat and fragile macro colonies lacking the structural characteristics of wild type colonies (Fig. 1C, Chan et al., 2014).

We investigated if and how overexpression of *ydaJKLMN* or of *ydaKLMN* effects biofilm formation in an *epsH* mutant background. For this reason, both overexpression constructs (pSG1164-PB53 and pSG1164-PB55) were introduced separately into the genome of an NCIB3610-derived *epsH* mutant and biofilm formation on solid MSgg medium was monitored 72 h post-inoculum in the presence and absence of 0.1 % xylose. As presented in Fig. 1C, an overexpression of the full length version *ydaJKLMN* (DS9259-PB53, *epsH*::*tet*, P_{xyl}-*ydaJKLMN*), resulted in an unstructured macro colony, similar to the parental strain (*epsH*::*tet*, DS9259, Chan *et al*., 2014). However, colonies harboring the pSG1164-PB53 construct (DS9259-PB53) revealed a noticeably different surface, a confined colony outline and a reduction in colony size in comparison to the *epsH* mutant, which exhibits small extensions at the periphery. In contrast to this, overexpression of *ydaKLMN* lacking *ydaJ*

caused wrinkled colony architecture, encompassing the formation of thick CR-accumulating wrinkles located around the center of the macro colony (DS9259-PB55, *epsH*::*tet*, P_{xyl}-*ydaKLMN*). The formation of these pronounced wrinkles in the absence of YdaJ accompanied by a reduction in colony size in the wild type backgrounds 168 and NCIB3610, respectively, reinforces a role of YdaJ in remodeling the putative extracellular sugar chains, synthesized most likely by the putative synthase-complex YdaM/YdaN, to form regular structures and to ensure structural integrity of the macro colony.

The putative c-di-GMP receptor YdaK is essential for the formation of the *ydaJKLMN*-related putative extracellular matrix component in *B. subtilis* 168 and NCIB 3610

In order to examine the potential YdaK dependence of the putative EPS machinery, we included a third overexpression construct in our study (pSG1164-PB56), which upon integration enables only the overexpression of the last 3 genes *ydaLMN*, whereas *ydaJK* are not expressed due to an inserted frame shift mutation in the pSG1164-PB56 construct. As illustrated in Fig. 2AB, an overexpression of *ydaLMN* in *B. subtilis* 168 and NCIB 3610 (fourth column, strains 168/NCIB3610-PB56, P_{xyl}-*ydaLMN*) resulted in similar phenotypes regarding CR-binding, cell aggregation and biofilm formation as observed for the corresponding parental wild type strains indicating that the unknown EPS is not synthesized in the absence of YdaK.

To verify this idea, we performed complementation assays using the overproduction strains *B. subtilis* 168/NCIB3610-PB56 (P_{xyl}-*ydaLMN*), and introduced a full-length copy of *ydaK* under the control of an IPTG-inducible promotor and a xylose dependent-promoter driving *ydaLMN*, respectively, at the *amyE* locus (strains 168-PB56+XG003/ PB16: P_{xyl}-*ydaLMN*; *amyE*::P_{IPTG}-*ydaK*/ *amyE*::P_{xyl}-*ydaK*). Expression of the ectopic *ydaK* gene upon addition of xylose (Fig. 2A, fifth column, P_{xyl}-*ydaLMN*; *amyE*::P_{xyl}-*ydaK*) or IPTG (Fig. 2C, third column, P_{xyl}-*ydaLMN*; *amyE*::P_{IPTG}-*ydaK*), restored CR-binding, wrinkle formation and cell aggregation of strain 168-PB55 overexpressing *ydaKLMN* from the original locus (Fig. 2A, third column, P_{xyl}-*ydaKLMN*), in contrast to the control strain which harbors a *yfp* gene at the *amyE* locus (strain 168 -PB56+pSG1193, P_{xyl}-*ydaLMN*; *amyE*::P_{xyl}-*yfp*).

Consistent with these results, a stable introduction of *ydaK* into the genome of *B. subtilis* NCIB 3610-PB56 and its expression (strain NCIB3610-PB56+PB16, P_{xyl}-*ydaLMN*; *amyE*::P_{xyl}-*ydaK*) also resulted in an altered biofilm development and formation, similar to that observed for strain NCIB 3610-PB55 (Fig. 2B, P_{xyl}-*ydaKLMN*), which leads to the conclusion that the putative c-di-GMP receptor YdaK is essential for the synthesis of the

unknown *ydaJKLMN*-related EPS in both *B. subtilis* backgrounds, and probably acts as an activating factor.

YdaK contains four transmembrane (-TM) α-helices and binds c-di-GMP via its soluble degenerated GGDEF domain. We wondered whether removal of the four TM-helices would influence the activity of YdaK reflected by CR binding of *B. subtilis* macro colonies. We therefore investigated an additional complementation strain, which contains a truncated version of *ydaK,* encoding for the soluble (degenerated) GGDEF domain at the *amyE* site under the control a xylose-inducible promotor, using the 168-PB56 background (Fig. 2C, fourth column, P_{xyl}-*ydaLMN*; *amyE*::P_{xyl}-$ydaK_{ggdef}$). The colony morphology of this strain (168-PB56+PB68) resembled that of wild type *B. subtilis* 168 and its derivative 168-PB56 (P_{xyl}-*ydaLMN*) and failed to restore the CR-binding wrinkled phenotype of strain 168-PB55 (P_{xyl}-*ydaKLMN*) indicating that YdaK needs to be embedded into the membrane via its TM domain in order to accomplish its biological function.

A functional YdaK-YFP fusion forms static subcellular clusters

Next, we wondered whether YdaK would be uniformly distributed around the cell membrane or whether it would cluster to specific sites. To investigate the subcellular localization of the putative c-di-GMP receptor YdaK via fluorescence microscopy (Fig. 3ABD), we first constructed a strain harboring a translational C-terminal YdaK-mVenus-YFP fusion, encoded at the original gene locus and expression of this fusion is driven by the natural promotor of the *ydaJ-N* operon in the *B. subtilis* 168 background (168-PB10*,* P_{sigB}-*ydaK-mVenus-yfp*).

Prior to the investigation of protein localization, we tested whether the fusion protein was biologically active (Fig. 3C). Because a deletion of any of the *ydaJKLMN* components has no obvious phenotype, we applied the same complementation assay as illustrated in Fig. 2, using strain 168-PB56 that overexpresses *ydaLMN* upon addition of xylose as a background to introduce a construct encoding *ydaK-mV-yfp* at the ectopic *amyE*-site under the control of *Pxyl* (168-PB56+PB57*,* P_{xyl}-*ydaLMN;* *amyE*::P_{xyl}-*ydaK-mVenus-yfp*). In contrast to the expression of a N-terminal mV-YFP-YdaK fusion, the expression of ectopic *ydaK-mV-yfp* together with an overexpression of *ydaLMN* resulted in a similar CR-binding phenotype as observed for the untagged version (strain 168-PB56+PB16, P_{xyl}-*ydaLMN;* *amyE*::P_{xyl}-*ydaK*), compare ii) & iv) in Fig. 3C) demonstrating that a C-terminal YFP-fusion can functionally replace the wild type protein.

YdaK-mV-YFP fusions, expressed under native circumstances, localized mostly as a single focus at the lateral cell membrane, but also as bright parallel double or single foci next

to or directly at the cell poles in exponentially growing cells (Fig. 3AB). We noticed that only a subset (18.5 +/- 1.3%, n= 1500) of cells exhibited fluorescent signals, suggesting that the expression of the *yda* operon occurs in only a subpopulation of cells. Overproduction of C-terminal CFP- or YFP fusions encoded *in trans* (amylase locus) under the control of an artificial promotor, resulted in a similar localization pattern upon addition of 0.1 % (v/v) xylose (Fig. 3D, strain 168-PB24, *amyE*::P_{xyl}-*ydaK-cfp*) as observed in case of YdaK-mVenus-YFP expressed from the endogenous locus (Fig. 3A, strain 168-PB10). Overproduction lead to an increased number of cells displaying foci (94.1 +/- 1.1%, n=400), and also in the number of foci per cells (62% of cells displayed 3 foci, only 5% in case of strain 168-PB10; n = 200); foci retained a preference of localization close to the cell poles and septa.

In summary, we show that the c-di-GMP effector YdaK forms static clusters at distinct sites of the cell membrane indicating that EPS production mediated by the YdaJ-N machinery may take place at single sites within the membrane of growing *B. subtilis* cells.

Components encoded within the *ydaJKLMN* operon co-localize to distinct sites of the cell membrane

We also localized other components encoded within the putative exopolysaccharide operon *ydaJKLMN*. Most fusions showed very low signals, which could only be resolved by using TIRF microscopy. We tagged each protein C-terminally with mV-YFP produced under the control of its original promoter. The plasmid-internal xylose-driven promoter ensured transcription of downstream genes. In case of YdaJ and YdaL fusions, we were not able to detect any membrane localization most likely due to missfolding of YFP outside the cytoplasm since the C-termini of the corresponding proteins are predicted to be outside. Localization attempts using mCherry as a fluorophore resulted in membrane localization but poor signal to noise ratios (data not shown). However, C-terminal YdaM-mYFP (Fig. 4B, strain 168-PB13, *ydaM-mV-yfp*) and YdaN-mV-YFP (Fig. 4C, strain 168-PB14, *ydaN-mV-yfp*) fusions resembled the pattern of YdaK-mV-YFP (strain 168-PB10) localization (Fig. 4A, left panels, snapshots) as well as the temporal behavior in exponentially growing 168 cells as presented in Fig. 4 (right panels). Again, only a subset of around 20% of cells (n=1400) displayed YdaM-mV-YFP and YdaN-mV-YFP signals, respectively. Time lapse microscopy over a period of 8 sec (continuous illumination with 515 nm, 100 ms intervals) of all three fusions revealed predominantly static localization of foci, at the same, mostly polar cellular positions (Fig. 4ABC, right panels; maximum intensity projections MIP and corresponding

kymographs). Interestingly, polar localization of bacterial exopolysaccharide producing machineries components has been reported for several bacterial species including *A. tumefaciens* (Xu et al., 2013), *E. coli* (Le Quere and Ghigo, 2009) and *S. coelicolor* (Xu et al., 2008).

Based on the observation of similar localization patterns, we wondered whether YdaK, YdaM and YdaN co-localize at the preferred cell regions. Using two different fluorophores and a 515 nm/445nm dual band filter, we found that 64.3 +/- 3.3 % of cells which expressed *ydaM-mV-yfp* from its original promotor and *ydaK-cfp* from the ectopic *amyE* locus displaced both signals (Fig. 5A), revealing predominant co-localization of both fusion proteins (n = 250, strain 168-PB13+24, *ydaM-mV-yfp; amyE*::P_{xyl}-*ydaK-cfp*). N-terminal mCerulean-YdaM (original locus) fusions also co-localized with C-terminal YdaK-mV-YFP fusions (ectopic locus) in 52.1 +/- 2.6 % of total cell counted (n=300, Fig. 5B, strain 168-PB93+PB57, P_{xyl}-*mcerulean-ydaM*; *amyE*::P_{xyl}-*ydaK-mV-yfp*). Additionally, we observed co-localization events between the putative exopolysaccharide synthase components mCerulean-YdaM (original locus) and YdaN-m-YFP (ectopic locus) in 57.8 +/- 4.3 % of cells displaying both foci (Fig. 5C, strain 168-PB93+PB96, P_{xyl}-*mcerulean-ydaM*; *amyE*::P_{xyl}-*ydaN-mV-yfp*).

In toto, we provide evidence that the putative EPS-synthase components YdaM and YdaN and the essential potential c-di-GMP receptor YdaK form static subcellular assemblies that localize preferentially at the bacterial cell poles and septa, similar to other bacterial exopolysaccharide machineries.

Discussion

The chemical composition of exopolysaccharide polymers produced by the soil bacterium *Bacillus subtilis* is presumably dependent on substrate availability and is currently mainly attributed to two transcriptional units: *epsA-O* & *sacB-yveB-yveA* (Branda et al., 2001; Chai et al., 2012; Dogsa et al., 2013). Our work suggests that *B. subtilis* possesses a third EPS operon, which must be taken into consideration in further studies regarding EPS production of exponential or stationary *B. subtilis* cultures. The most likely function of the *ydaJKLMN* operon is the synthesis of an exopolysaccharide, because in addition to the effect of increased CR binding and wrinkle formation (plus reduced spreading diameter of colonies) during biofilm formation, induction of the operon leads to cell clumping during exponential growth. In spite of our best efforts, we have not found the exact physiological role of the *yda* operon. The transcriptional unit is assigned to the *B. subtilis* σ^B- regulon (Nicolas et al., 2012), but deletion mutants did not reveal any phenotype in biofilm formation or stress resistance, and overproducing the operon did not increase e.g. ethanol stress resistance (data not shown). We can therefore only speculate that the putative exopolysaccharide provides stress resistance under specific stress conditions, and/or under extreme stress, or under unknown conditions.

However, using complementation strains and CR binding assays of *B. subtilis* macro colonies, we show that *ydaK* expression is essential for the activation of the putative exopolysaccharide synthesizing components. YdaK contains four predicted N-terminal transmembrane helices and a soluble degenerate GGDEF domain, which is not able to synthesize but is able to bind the second messenger c-di-GMP with moderate affinity (dissociation constant 1.1 µM), most likely at the so-called I-site (Gao et al., 2013). The role of c-di-GMP, known to be a positive regulator of ECM production, during *B. subtilis* biofilm formation has been addressed by two recent studies (Chen et al., 2012; Gao et al. 2013).

No obvious consequence on biofilm formation by changes in intracellular c-di-GMP was observed, whereas high c-di-GMP resulted in motility inhibition via the conserved PilZ-domain protein DgrA (dissociation constant 11.0 µM). Interestingly, Gao et al. were unable to detect c-di-GMP in WT cells indicating very low concentrations under their growth conditions (limit of detection 50 pg/µL). Low intracellular c-di-GMP concentrations do not necessarily exclude the potential of c-di-GMP to activate a corresponding low-affinity receptor such as YdaK. The "local signaling/pool" hypothesis i.a. proposes spatial proximity of c-di-GMP metabolizing proteins, effectors and targets producing small localized specific concentrations as suggested in several studies (Merritt et al., 2010; Dahlstrom et al., 2015). Therefore, *B. subtilis* may employ a c-di-GMP signaling network for the regulation of the *yda*

operon via a degenerated GGDEF – TM protein to positively regulate extracellular matrix formation and thus possibly biofilm formation. *B. subtilis* harbors a minimalistic set of three diguanylate cyclases: DgcK, DgcP and DgcW, which can potentially contribute to the c-di-GMP pool utilized by YdaK and/ or serve as interaction partners in order to activate EPS production. In this study, we provide a new tool to study the role of c-di-GMP during biofilm formation in the model organism *B. subtilis*.

Importantly, we observed the formation of subcellular clusters (usually one per cell) of YdaK, YdaM and YdaN at distinct sites (with an enrichment at the cell poles) of exponentially growing *B. subtilis* cells using fluorescence microscopy. The clusters showed static localization, possibly because the synthetase components are anchored within the cell membrane (as predicted by bioinformatics tools, see supplementary material). Co-localization events of YdaM/YdaK and YdaM/ YdaN fluorescent fusions support the idea that subcellular localization at the cell membrane might be important for facilitating protein-protein interactions. This idea is further supported by the observation that a YdaK variant lacking the TM domain is unable to support the activity of the other Yda proteins.

In summary, our observations of clustered components of a putative exopolysaccharide machinery reveal that the concept of enzymatic subcellular assemblies within the membrane of enzymes whose product is secreted is wide spread, and *B. subtilis* contains at least two of such assemblies, the YdaJKLMN machinery and the bacillaene synthase cluster (Straight et al., 2007). It will be highly interesting to further investigate which c-di-GMP pathway activates the Yda proteins, and how the assembly is restricted to a single site within the cell membrane of a bacterium.

Acknowledgments

We would like to thank Luise Kleine Borgmann from the Gurol Süel laboratory (UCSD) for the Biofilm protocol, Felix Dempwolff (now University of Indiana) for help with confocal microscopy and for helpful discussions. Thomas Rösch (University of Marburg) helped with Fig S2, Daniel Kearns and Charles Dann III (University of Indiana, USA) provided strains, which is gratefully acknowledged. Gert Bange (SYNMIKRO, Marburg) provided helpful comments on the manuscript. This work was supported by the state of Hessen (LOEWE program, SYNMIKRO), and by the University of Marburg.

References

Asally, M., Kittisopikul, M., Rue, P., Du, Y., Hu, Z., Cagatay, T. et al. (2012) Localized cell death focuses mechanical forces during 3D patterning in a biofilm. *Proc Natl Acad Sci U S A* **109**: 18891-18896.

Branda, S.S., Gonzalez-Pastor, J.E., Ben-Yehuda, S., Losick, R., and Kolter, R. (2001) Fruiting body formation by Bacillus subtilis. *Proc Natl Acad Sci U S A* **98**: 11621-11626.

Branda, S.S., Chu, F., Kearns, D.B., Losick, R., and Kolter, R. (2006) A major protein component of the Bacillus subtilis biofilm matrix. *Mol Microbiol* **59**: 1229-1238.

Cairns, L.S., Hobley, L., and Stanley-Wall, N.R. (2014) Biofilm formation by Bacillus subtilis: new insights into regulatory strategies and assembly mechanisms. *Mol Microbiol* **93**: 587-598.

Campbell, A., Berg, D.E., Botstein, D., Lederberg, E.M., Novick, R.P., Starlinger, P., and Szybalski, W., "", " 1977, ; also, 1979, Gene, 5, 197 - 206 (1977) Nomenclatur of transposable elemetns in prokaryotes In *DNA Insertion Elements, Plasmids and Episomes*. Bukhari, A.I., Shapiro, J.A., and Adhya, S.L. (eds): Cold Spring Harbor, New York, pp. 15-22.

Chai, Y., Beauregard, P.B., Vlamakis, H., Losick, R., and Kolter, R. (2012) Galactose metabolism plays a crucial role in biofilm formation by Bacillus subtilis. *MBio* **3**: e00184-00112.

Chan, J.M., Guttenplan, S.B., and Kearns, D.B. (2014) Defects in the flagellar motor increase synthesis of poly-gamma-glutamate in Bacillus subtilis. *J Bacteriol* **196**: 740-753.

Chen, L.H., Koseoglu, V.K., Guvener, Z.T., Myers-Morales, T., Reed, J.M., D'Orazio, S.E. et al. (2014) Cyclic di-GMP-dependent signaling pathways in the pathogenic Firmicute Listeria monocytogenes. *PLoS Pathog* **10**: e1004301.

Chen, Y., Chai, Y., Guo, J.H., and Losick, R. (2012) Evidence for cyclic Di-GMP-mediated signaling in Bacillus subtilis. *J Bacteriol* **194**: 5080-5090.

Costerton, J.W., Lewandowski, Z., Caldwell, D.E., Korber, D.R., and Lappin-Scott, H.M. (1995) Microbial biofilms. *Annu Rev Microbiol* **49**: 711-745.

Dahlstrom, K.M., Giglio, K.M., Collins, A.J., Sondermann, H., and O'Toole, G.A. (2015) Contribution of Physical Interactions to Signaling Specificity between a Diguanylate Cyclase and Its Effector. *MBio* **6**: e01978-01915.

Dogsa, I., Brloznik, M., Stopar, D., and Mandic-Mulec, I. (2013) Exopolymer diversity and the role of levan in Bacillus subtilis biofilms. *PLoS One* **8**: e62044.

Flemming, H.C., and Wingender, J. (2010) The biofilm matrix. *Nat Rev Microbiol* **8**: 623-633.

Friedman, L., and Kolter, R. (2004) Genes involved in matrix formation in Pseudomonas aeruginosa PA14 biofilms. *Mol Microbiol* **51**: 675-690.

Gao, X., Mukherjee, S., Matthews, P.M., Hammad, L.A., Kearns, D.B., and Dann, C.E., 3rd (2013) Functional characterization of core components of the Bacillus subtilis cyclic-di-GMP signaling pathway. *J Bacteriol* **195**: 4782-4792.

Hengge, R. (2009) Principles of c-di-GMP signalling in bacteria. *Nat Rev Microbiol* **7**: 263-273.

Hobley, L., Ostrowski, A., Rao, F.V., Bromley, K.M., Porter, M., Prescott, A.R. et al. (2013) BslA is a self-assembling bacterial hydrophobin that coats the Bacillus subtilis biofilm. *Proc Natl Acad Sci U S A* **110**: 13600-13605.

Jenal, U., and Malone, J. (2006) Mechanisms of cyclic-di-GMP signaling in bacteria. *Annu Rev Genet* **40**: 385-407.

Kobayashi, K., and Iwano, M. (2012) BslA(YuaB) forms a hydrophobic layer on the surface of Bacillus subtilis biofilms. *Mol Microbiol* **85**: 51-66.

Koseoglu, V.K., Heiss, C., Azadi, P., Topchiy, E., Guvener, Z.T., Lehmann, T.E. et al. (2015) Listeria monocytogenes exopolysaccharide: origin, structure, biosynthetic machinery and c-di-GMP-dependent regulation. *Mol Microbiol* **96**: 728-743.

Le Quere, B., and Ghigo, J.M. (2009) BcsQ is an essential component of the Escherichia coli cellulose biosynthesis apparatus that localizes at the bacterial cell pole. *Mol Microbiol* **72**: 724-740.

Lee, V.T., Matewish, J.M., Kessler, J.L., Hyodo, M., Hayakawa, Y., and Lory, S. (2007) A cyclic-di-GMP receptor required for bacterial exopolysaccharide production. *Mol Microbiol* **65**: 1474-1484.

Lewis, P.J., and Marston, A.L. (1999) GFP vectors for controlled expression and dual labelling of protein fusions in Bacillus subtilis. *Gene* **227**: 101-110.

Liang, Z.X. (2015) The expanding roles of c-di-GMP in the biosynthesis of exopolysaccharides and secondary metabolites. *Nat Prod Rep* **32**: 663-683.

Marvasi, M., Visscher, P.T., and Casillas Martinez, L. (2010) Exopolymeric substances (EPS) from Bacillus subtilis: polymers and genes encoding their synthesis. *FEMS Microbiol Lett* **313**: 1-9.

McLoon, A.L., Guttenplan, S.B., Kearns, D.B., Kolter, R., and Losick, R. (2011) Tracing the domestication of a biofilm-forming bacterium. *J Bacteriol* **193**: 2027-2034.

Merritt, J.H., Ha, D.G., Cowles, K.N., Lu, W., Morales, D.K., Rabinowitz, J. et al. (2010) Specific control of Pseudomonas aeruginosa surface-associated behaviors by two c-di-GMP diguanylate cyclases. *MBio* **1**.

Morikawa, M., Kagihiro, S., Haruki, M., Takano, K., Branda, S., Kolter, R., and Kanaya, S. (2006) Biofilm formation by a Bacillus subtilis strain that produces gamma-polyglutamate. *Microbiology* **152**: 2801-2807.

Nagorska, K., Ostrowski, A., Hinc, K., Holland, I.B., and Obuchowski, M. (2010) Importance of eps genes from Bacillus subtilis in biofilm formation and swarming. *J Appl Genet* **51**: 369-381.

Nicolas, P., Mader, U., Dervyn, E., Rochat, T., Leduc, A., Pigeonneau, N. et al. (2012) Condition-dependent transcriptome reveals high-level regulatory architecture in Bacillus subtilis. *Science* **335**: 1103-1106.

Robledo, M., Jimenez-Zurdo, J.I., Velazquez, E., Trujillo, M.E., Zurdo-Pineiro, J.L., Ramirez-Bahena, M.H. et al. (2008) Rhizobium cellulase CelC2 is essential for primary symbiotic infection of legume host roots. *Proc Natl Acad Sci U S A* **105**: 7064-7069.

Romero, D., Aguilar, C., Losick, R., and Kolter, R. (2010) Amyloid fibers provide structural integrity to Bacillus subtilis biofilms. *Proc Natl Acad Sci U S A* **107**: 2230-2234.

Roux, D., Cywes-Bentley, C., Zhang, Y.F., Pons, S., Konkol, M., Kearns, D.B. et al. (2015) Identification of Poly-N-acetylglucosamine as a Major Polysaccharide Component of the Bacillus subtilis Biofilm Matrix. *J Biol Chem* **290**: 19261-19272.

Scoffone, V., Dondi, D., Biino, G., Borghese, G., Pasini, D., Galizzi, A., and Calvio, C. (2013) Knockout of pgdS and ggt genes improves gamma-PGA yield in B. subtilis. *Biotechnol Bioeng* **110**: 2006-2012.

Shapiro, J.A. (1998) Thinking about bacterial populations as multicellular organisms. *Annu Rev Microbiol* **52**: 81-104.

Simm, R., Morr, M., Kader, A., Nimtz, M., and Romling, U. (2004) GGDEF and EAL domains inversely regulate cyclic di-GMP levels and transition from sessility to motility. *Mol Microbiol* **53**: 1123-1134.

Solano, C., Garcia, B., Latasa, C., Toledo-Arana, A., Zorraquino, V., Valle, J. et al. (2009) Genetic reductionist approach for dissecting individual roles of GGDEF proteins within the c-di-GMP signaling network in Salmonella. *Proc Natl Acad Sci U S A* **106**: 7997-8002.

Stewart, P.S., and Franklin, M.J. (2008) Physiological heterogeneity in biofilms. *Nat Rev Microbiol* **6**: 199-210.

Straight, P.D., Fischbach, M.A., Walsh, C.T., Rudner, D.Z., and Kolter, R. (2007) A singular enzymatic megacomplex from Bacillus subtilis. *Proc Natl Acad Sci U S A* **104**: 305-310.

Vlamakis, H., Chai, Y., Beauregard, P., Losick, R., and Kolter, R. (2013) Sticking together: building a biofilm the Bacillus subtilis way. *Nat Rev Microbiol* **11**: 157-168.

Xu, H., Chater, K.F., Deng, Z., and Tao, M. (2008) A cellulose synthase-like protein involved in hyphal tip growth and morphological differentiation in streptomyces. *J Bacteriol* **190**: 4971-4978.

Xu, J., Kim, J., Koestler, B.J., Choi, J.H., Waters, C.M., and Fuqua, C. (2013) Genetic analysis of Agrobacterium tumefaciens unipolar polysaccharide production reveals complex integrated control of the motile-to-sessile switch. *Mol Microbiol* **89**: 929-948.

Zeigler, D.R., Pragai, Z., Rodriguez, S., Chevreux, B., Muffler, A., Albert, T. et al. (2008) The origins of 168, W23, and other Bacillus subtilis legacy strains. *J Bacteriol* **190**: 6983-6995.

Legends to the figures

Fig. 1. Congo Red staining, aggregative behavior and biofilm surface architecture of macro colonies overexpressing the putative exopolysaccharide operon variants *ydaJKLMN* and *ydaKLMN* in different genomic *B. subtilis* backgrounds

(**A**) Exopolysaccharide-dependent *B*. subtilis 168 cell-aggregation in liquid LB medium supplemented with 0.1 % (v/v) xylose and CR-binding of macro colonies of parental WT *B. subtilis* 168 and strains carrying integrated overexpression constructs as illustrated in Fig. S2: WT *B. subtilis* 168 (**I**. P_{sigB}-*ydaJKLMN*), 168-PB53 (**II**. P_{xyl}-*ydaJKLMN)*, 168-PB55 (**III**. P_{xyl}-*ydaKLMN*) and 168-PB55+PB15 (**IV**. P_{xyl}-*ydaKLMN*; *amyE*::P_{xyl}-*ydaJ*). Individual clones of WT 168 and the indicated overproduction strains were grown in LB to mid-log phase and spotted on indicator plates supplemented with or without 0.1 % (v/v) xylose, CR 40 µg/ml, CB 20 µg/ml, following an incubation of 24 h at 37 °C before imaging colony morphology. Scale bar: 2.5 mm (**B**) Effect of *ydaJKLMN*/ *ydaKLMN* overexpression and *ydaK* deletion on colony surface architectures of *B. subtilis* NCIB3610 using biofilm-promoting medium. An aliquot of exponentially growing cells was washed once in MSgg liquid medium and incubated for additional 30 min in MSgg at 37°C before spotting the indicated strains on MSgg agar plates (+/- 0.1 % (v/v) xylose, 20 µg/ml CR & CB) followed by an incubation of 72 h at 25 °C. Strains: WT *B. subtilis* NCIB3610 (P_{sigB}-*ydaJKLMN*), NCIB3610-PB53 (P_{xyl}-*ydaJKLMN*), NCIB3610-PB55 (P_{xyl}-*ydaKLMN*), NCIB3610-DS9289 (Δ*ydaK*, Gao *et al*., 2013). Scale bar represents 5 mm. (**C**) Effect of *ydaJKLMN*/ *ydaKLMN* overexpression on colony surface architecture in a NCIB3610-derived *epsH* biofilm deficient mutant using the biofilm-promoting medium MSgg. Strains: *sinR*::*kan* (DS859, Blair *et al*., 2008; reflects overproduction of *epsA-O* derived exopolysaccharide), *epsH*::*tet* (DS9259, Chan *et al*., 2014), DS9259-PB53 (*epsH*::*tet*; P_{xyl}-*ydaJKLMN*), DS9259-PB55 (*epsH*::*tet*; P_{xyl}-*ydaKLMN*). Experimental setup as described in (B). Scale bar: 5 mm.

Fig. 2. The synthesis of the *ydaJKLMN*-related unknown EPS depends on the presence of the potential c-di-GMP receptor and 4TM protein YdaK in *B. subtilis*

(**A**) CR-staining of wild type strain *B. subtilis* 168 (P_{sigB}-*ydaJKLMN*) and its derivatives *B. subtilis* 168-PB53 (P_{xyl}-*ydaJKLMN)*, 168-PB55 (P_{xyl}-*ydaKLMN)*, 168-PB56 (P_{xyl}-*ydaLMN*), 168-PB56+PB16 (P_{xyl}-*ydaLMN*; *amyE*::P_{xyl}-*ydaK*), 168-PB56+pSG1193NLMV (P_{xyl}-*ydaLMN*; *amyE*::P_{xyl}-*yfp*). Experimental as described above. (**B**) Top view of *B. subtilis* biofilm morphology on MSgg solid medium at different time points for wild type strain NCIB 3610 (DK1042), the overproduction mutant strains NCIB3610-PB53 (P_{xyl}-*ydaJKLMN)*, -PB55 (P_{xyl}-*ydaKLMN)*, -PB56 (P_{xyl}-*ydaLMN*) and the complementation strains NCIB3610-

PB56+PB16 (P_{xyl}-*ydaLMN*; *amyE*::P_{xyl}-*ydaK*) and NCIB3610-PB56+pSG1193NLMV (P_{xyl}-*ydaLMN*; *amyE*::P_{xyl}-*yfp*). Experimental setup as described above. **(C)** CR-binding phenotypes of the parental WT *B. subtilis* 168 (P_{sigB}-*ydaJKLMN*) and strains carrying integrated overexpression constructs pPB55 (P_{xyl}-*ydaKLMN*), pPB56+pXG003 (P_{xyl}-*ydaLMN*; *amyE*::P_{IPTG}-*ydaK*), pPB56+pPB68 (P_{xyl}-*ydaLMN*; *amyE*::P_{xyl}-*ydaK*$_{ggdef}$), pPB16 (*amyE*::P_{xyl}-*ydaK*) and pXG003 (*amyE*::P_{IPTG}-*ydaK*; Gao *et al*., 2013) respectively. Scale bars represent 5 mm.

Fig. 3. Subcellular localization and dynamics of the putative c-di-GMP receptor YdaK during exponential growth in live *B. subtilis* 168 cells using confocal fluorescence microscopy

(**A**) Exponentially growing cells expressing *ydaK-mV-yfp* from the original locus in the presence of 0.1 % (v/v) xylose to ensure transcription of downstream genes (strain 168-PB10). Overlay of Normarski DIC and YFP-fluorescence. Bar, 2 µm (**B**) Corresponding time-lapse microscopy experiment of YdaK-mVenus-YFP. Images were captured at the time points (seconds) indicated inside the panels. Bar, 2 µm (**C**) Verification of YdaK-mV-YFP functionality by CR-staining in the presence of 0.1 % (v/v) xylose **i**) WT *B. subtilis* 168 (P_{sigB}-*ydaJKLMN*) **ii**) 168-PB56+PB16 (P_{xyl}-*ydaLMN*; *amyE*::P_{xyl}-*ydaK*) **iii**) 168-PB56+pSG1193NLMV (P_{xyl}-*ydaLMN*; *amyE*::P_{xyl}-*mV-yfp*) **iv**) 168-PB56+PB57 (P_{xyl}-*ydaLMN*; *amyE*::P_{xyl}-*ydaK-mV-yfp*). Bar, 5 mm (**D**) Mid-exponential-phase *B. subtilis* 168 cells expressing *ydaK-cfp* the amylase locus, 45 min after induction with 0.1 % (v/v) xylose (strain 168-PB24). Bar, 2 µm

Fig. 4. Subcellular localization of components of the putative YdaJ-N exopolysaccharide machinery

Fluorescence microscopy of endogenously expressed *ydaK-mV-yfp* (**A**), *ydaM-mV-yfp* (**B**) and *ydaN-mV-yfp* (**C**) in exponentially growing *B. subtilis* 168 cells and corresponding bright field images (left panel). Right panel: maximum intensity projections (MIP) from timelapse microscopy and kymographs showing the motion of individual particles over time. Strains: 168-PB10 (*ydaK-mV-yfp*), -PB13 (*ydaM-mV-yfp*), - PB14 (*ydaN-mV-yfp*). Data are representatives of two biolgical replicates. Bars, 2 µm.

Fig. 5. Simultaneous localization of the potential c-di-GMP receptor YdaK and associated putative polysaccharide synthase components YdaM and YdaN

(**A**) Exponential *B. subtilis* 168 cells producing YdaM-mV-YFP (original locus and promotor, false colored green) and YdaK-CFP (ectopic locus, xylose-inducible promotor, false colored red). Triangles in the overlays of corresponding pictures (right panels) indicate colocalization or close proximity of foci. Strain: 168-PB10+PB24. (**B**) Colocalization of mCerulean-YdaM (original locus, xylose-inducible promotor, false colored green) and YdaK-mV-YFP (ectopic locus, xylose-inducible promotor, false colored red). Strain: 168-PB93+PB57. (**C**) Colocalization of mCerulean-YdaM (original locus, xylose-inducible promotor, false colored green) and YdaN-mV-YFP (ectopic locus, xylose-inducible promotor, false colored red). Strain: 168-PB93+PB96. Scale bars: 2 μm; BF: brightfield

Supplemental Material

Text S1
Bioinformatic analysis of components encoded within the *ydaJKLMN* operon
Text S2
Experimental procedures
Fig. S1. Condition-dependent transcriptomes of *ydaJ*, *ydaK*, *ydaL*, *ydaM, ydaN* and of the 5′ upstream region
Fig. S2.
Hypothetical model for the putative *ydaJKLMN* encoded exopolysaccharide synthesis machinery
Fig. S3.
EPS-dependent *B. subtilis* cell aggregation measured by spectrophotometry
Table S1/ S2/ S3
Oligonucleotides/ vectors and plasmids/ strains used in this study

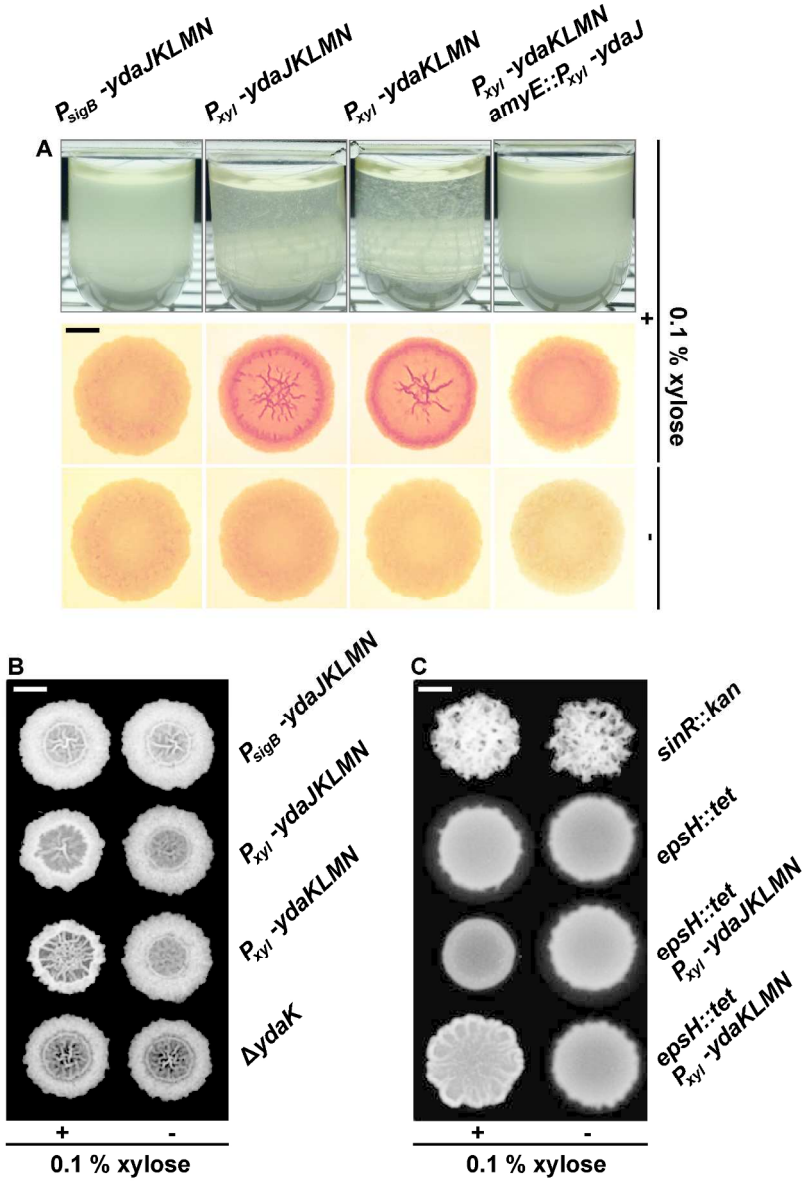

Congo Red staining, aggregative behavior and biofilm surface architecture of macro colonies overexpressing the putative exopolysaccharide operon variants *ydaJKLMN* and *ydaKLMN* in different genomic *B. subtilis* backgrounds

Fig. 1

184x271mm (300 x 300 DPI)

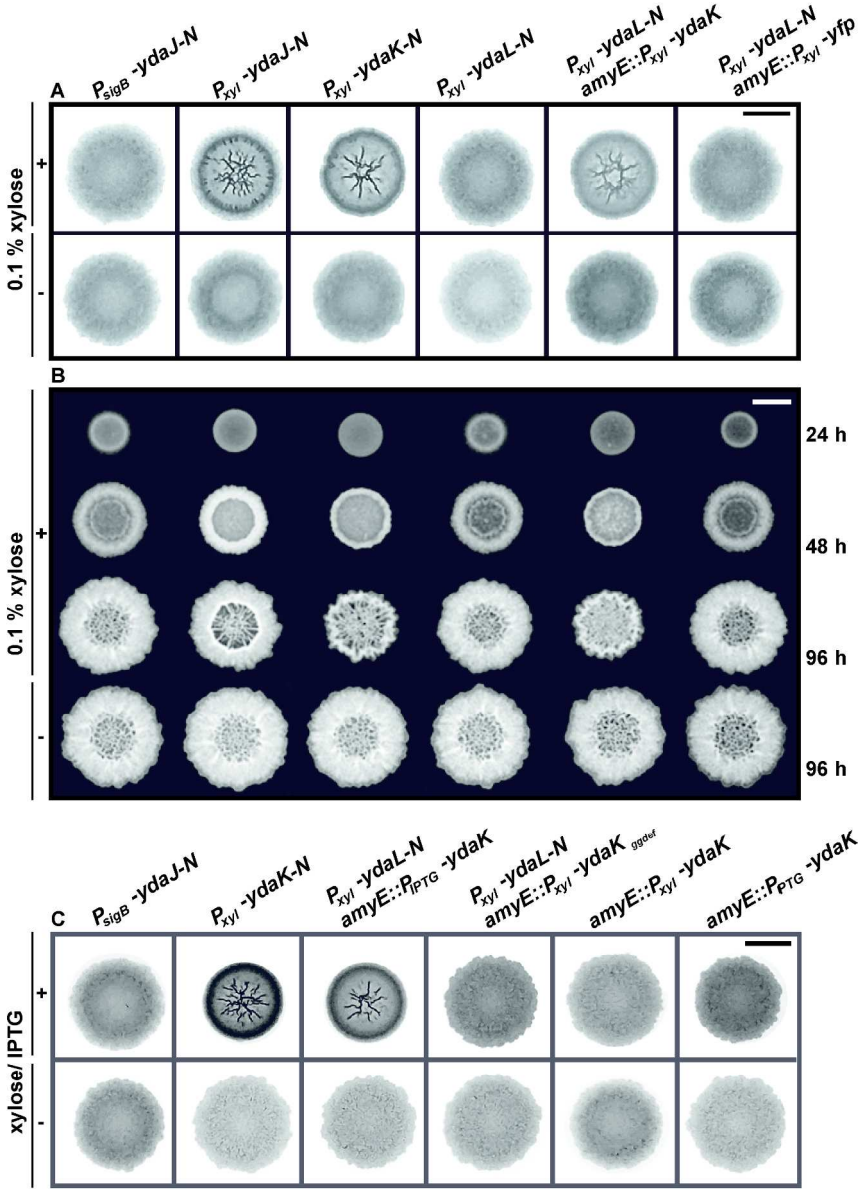

The synthesis of the *ydaJKLMN*-related unknown EPS depends on the presence of the potential c-di-GMP receptor and 4TM protein YdaK in *B. subtilis*
Fig. 2
201x277mm (300 x 300 DPI)

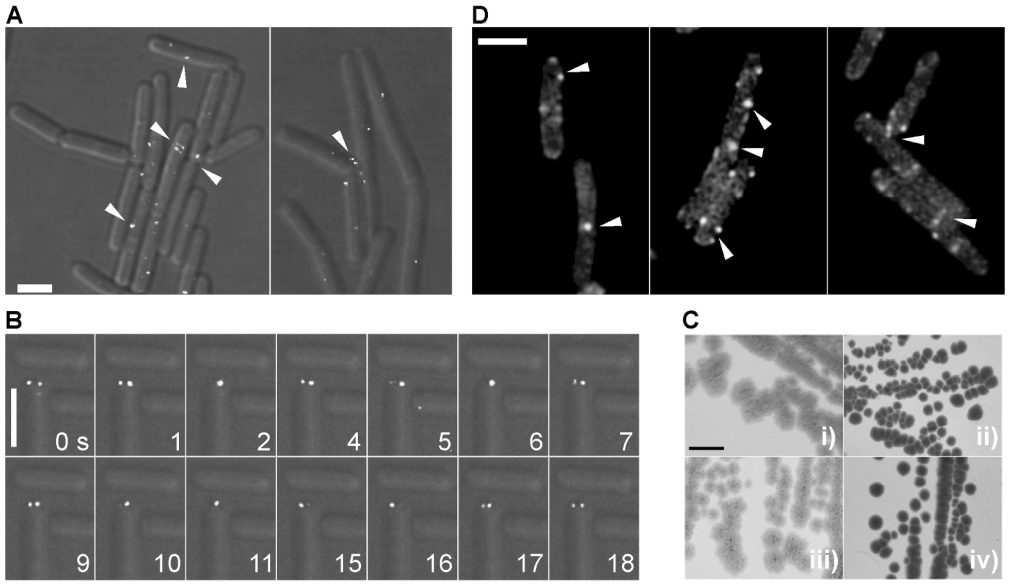

Subcellular localization and dynamics of the putative c-di-GMP receptor YdaK during exponential growth in live *B. subtilis* 168 cells using confocal fluorescence microscopy
Fig. 3
188x108mm (300 x 300 DPI)

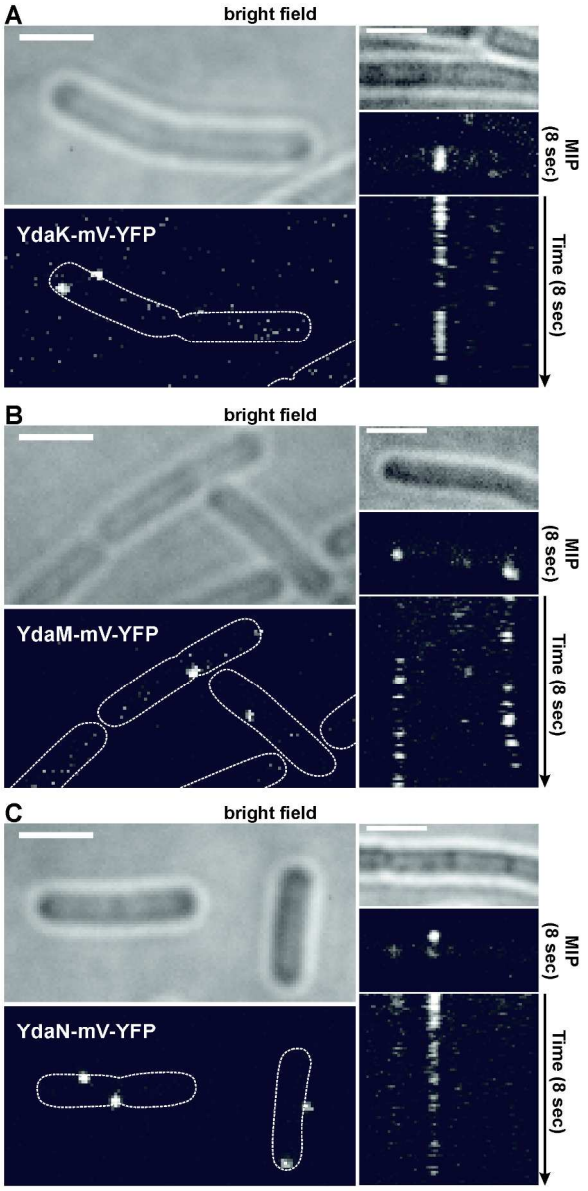

Subcellular localization of components of the putative YdaJ-N exopolysaccharide machinery
Fig. 4
140x282mm (300 x 300 DPI)

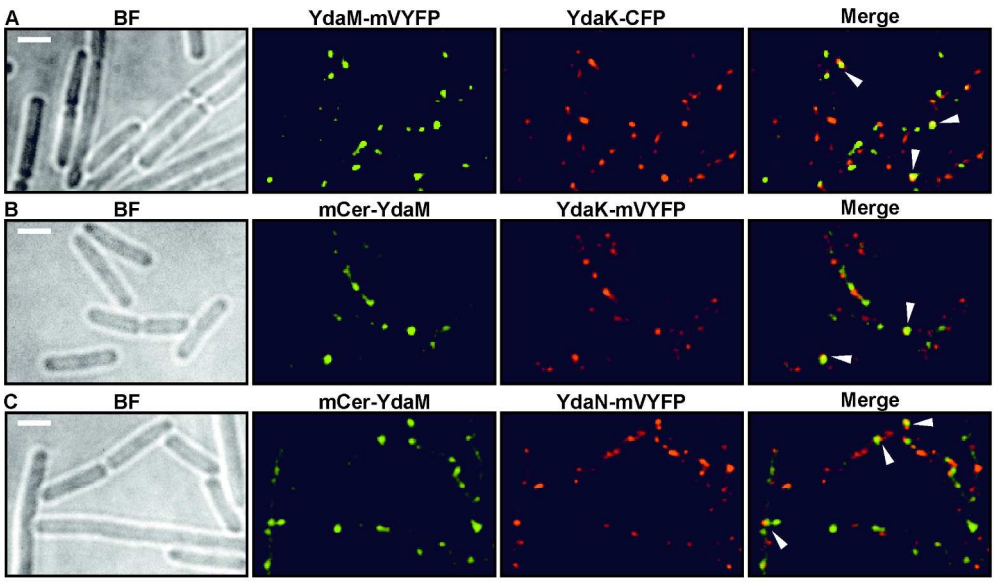

Simultaneous localization of the potential c-di-GMP receptor YdaK and associated putative polysaccharide synthase components YdaM and YdaN
Fig. 5
209x121mm (300 x 300 DPI)